Formation of Porous Pt Nanoparticles through Core–Shell Pt–Al Nanoalloys and Wet Chemical Etching

Zhongrong Shen,*[1,2] Yasuo Matsuki,[2,3] Koichi Higashimine,[4] Mikio Miyake,[5] and Tatsuya Shimoda*[2,5]

[1]*Green Devices Research Center, Japan Advanced Institute of Science and Technology,*
1-1 Asahidai, Nomi, Ishikawa 923-1292

[2]*Shimoda Nano Liquid Process Project, ERATO, Japan Science and Technology Agency,*
2-5-3 Asahidai, Nomi, Ishikawa 923-1211

[3]*Yokkaichi Research Center, JSR Corporation, 100 Kawajiri-cho, Yokkaichi, Mie 510-8552*

[4]*Center for Nano Materials and Technology, Japan Advanced Institute of Science and Technology,*
*1-1 Asahidai, Nomi, Ishikawa 923-1292*

[5]*School of Materials Science, Japan Advanced Institute of Science and Technology,*
1-1 Asahidai, Nomi, Ishikawa 923-1292

(Received March 21, 2012; CL-120243; E-mail: z-shen@jaist.ac.jp, tshimoda@jaist.ac.jp)

We introduce a strategy for preparation of porous Pt nanoparticles with high catalytic activity and large surface area by changing the morphology of large-sized Pt nanoparticle into Pt–Al nanoalloy, then following a simple wet-chemical etching to remove partial Al.

Platinum (Pt) nanoparticles that combine size- and shape-dependent physicochemical properties are preferable for catalysis and sensor applications.[1] An important issue relating to their application is how to reduce the amount of Pt used while preserving high catalytic activity of Pt. Fundamental studies of single-crystal surfaces of bulk or large-sized Pt nanocrystals have shown that high-index planes generally exhibit much higher catalytic activity than that of the most common stable planes, such as {111}, {100}, and even {110}. High-index planes have a high density of atomic steps, ledges, and kinks, which usually serve as active sites for breaking chemical bonds.[2] However, it is rather difficult to synthesize Pt nanoparticles by crystal growth that combine both large surface area and the desired highly active facets because Pt nanoparticles <5 nm in size tend to exist as truncated octahedrons covered by a mixture of {111} and {100} facets for minimizing the total interfacial free energy.[3] Until now, only Zhou and co-workers have reported synthesis of high-index-faceted Pt nanocrystals supported on carbon black with sizes of 2–10 nm by using a square-wave potential method.[4] It is still a challenge to prepare small-sized Pt nanocrystals with high-index facets by crystal growth. Dealloying is a candidate to prepare high-index surfaces instead of crystal growth because different atom-packing structures are formed during the wet-chemical etching. However, there are few reports based on this method for preparing porous Pt nanoparticles with larger surface area and catalytic activity.

Here for producing porous nanostructures, we first introduce a novel strategy to prepare porous Pt nanoparticles with large surface area by changing the morphology of large-sized Pt nanoparticles. The method provides good size and shape control as well as clean surfaces by a direct, template-free route and generates porosity by simple chemical etching (Figure 1). Porous Pt nanoparticles exhibit catalytic activities different from their solid counterparts with the advantages of low density, material savings, and reduced costs.[5] Considering that a porous Pt structure cannot form on small nanoparticles because they
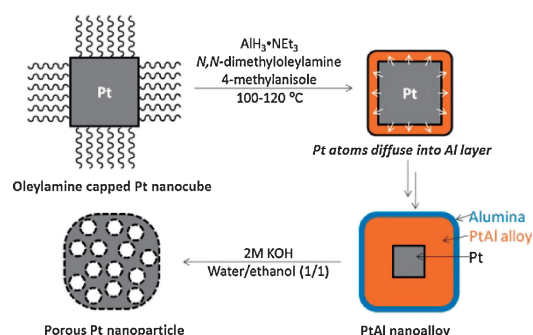
Figure 1. Schematic illustration of synthesizing porous Pt nanoparticle from Pt nanocube.

shrink to single crystals owning to the strong internal strain energy of Pt,[6] we employed one large-sized Pt nanocube with a diameter of 30–40 nm as the Pt source based on our recent work.[1d] Then we used the following two critical strategies to realize the porous nanostructure. The first is to grow Al on Pt nanocrystals in the presence of triethylamine alane (AlH_3NEt_3). We add excess *N,N*-dimethyloctylamine (bp 195 °C) to prevent AlH_3NEt_3 from polymerizing at high temperature when triethylamine evaporates. In the experiment, Pt serves not only as a catalyst of dehydrogenation of alane but also as a seed for Al crystallization. Concurrently, Pt diffuses into the Al layer to form Pt–Al nanoalloys. This is probably because both Al and Pt have the same face-centered cubic (fcc) structures and almost equal atomic radii (Al: 1.43 Å; Pt: 1.39 Å) and lattice constants (Al: 4.05 Å; Pt: 3.92 Å), making it easier to incorporate Al atoms into a Pt lattice. The second strategy is to partially remove Al by chemical etching in an acidic or an alkaline solution.

For a typical reaction, a 10 mg of Pt nanocube was dispersed in 6 mL of 4-methylanisole (bp 174 °C) by sonication. In a glovebox with less than 1 ppm O_2, 0.2 mL of alane (excess, $Al/Pt_{atomic} \approx 20/1$) and 0.2 mL of *N,N*-dimethyloctylamine were added into the Pt nanocube solution. Then the reaction system was heated to 110–120 °C on a hot plate. Bubbles appeared when the reaction temperature approached 100 °C. The reaction continued for 1–3 h, and then the system was allowed to cool on standing to room temperature. The precipitate, Pt–Al nanoalloy, was washed first with dehydrated toluene and then with ethanol. To prepare porous Pt nanoparticles, 10 mg of Pt–Al nanoalloy
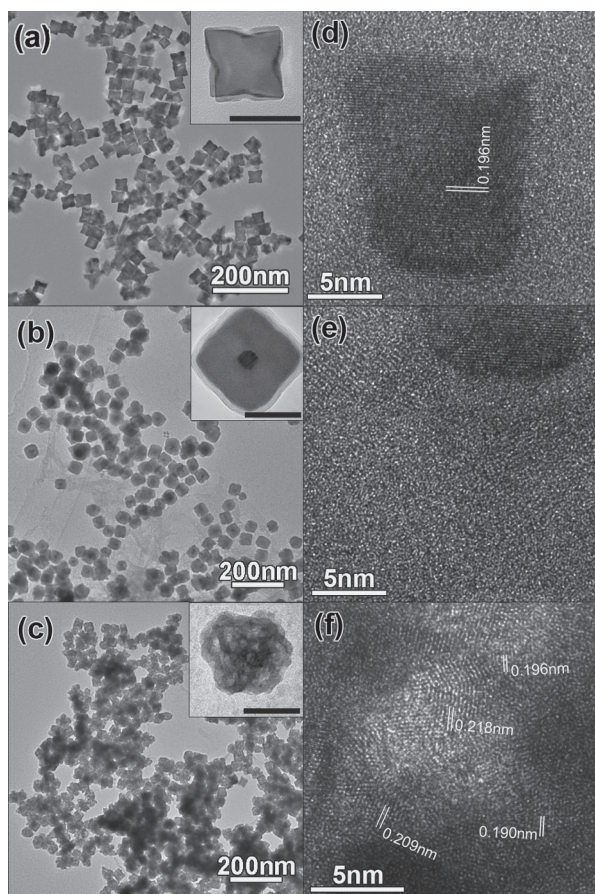
Figure 2. (a–c) TEM images of evolution from Pt nanocube to porous Pt nanoparticle: (a) oleylamine-capped Pt nanocubes, (b) Pt–Al nanoalloys after depositing Al on Pt nanocubes, and (c) porous Pt nanoparticles after partially removing Al from Pt–Al nanoalloys by KOH solution. Insets show the enlarged particles (the scale bar is 30 nm). (d–f) Atomic resolution TEM images of core–shell Pt–Al nanoalloy and porous Pt nanoparticles: (d) core of the core–shell Pt–Al nanoalloy, (e) shell of the core–shell Pt–Al nanoalloy, (f) one pore of the porous Pt nanoparticle.

was dispersed into 5 mL of ethanol by sonication, and then 5 mL of 2 M aqueous KOH solution was added to remove Al and aluminium oxide. Bubbles appeared after adding KOH, indicating Al dissolution and H_2 emission. The reaction continued overnight, and then the solution was centrifuged and washed with an excess of ethanol/water (1:1) mixture. No potassium (K) signal can be detected from the energy-dispersive X-ray spectroscopy (EDX) spectrum (Figure S1).

The overall synthetic result is shown in Figure 2. We synthesized large-sized Pt nanocubes with a diameter of 30–40 nm according to our previous research (Figure 2a).[1d] After triethylamine alane treatment for 2 h, the diameter of the nanocrystals increased to 53 nm, as shown in Figure 2b. To elucidate the formation process of the Pt–Al nanoalloy, we monitored the growth by transmission electron microscopy (TEM) at deposition times of 1 and 2 h as shown in Supporting Information (Figure S2).[8] The diameter of the particles increased, accompanied by a decrease in core size, indicating that Pt

atoms diffused into the Al layer to form a Pt–Al nanoalloy. The synthesized Pt–Al nanoalloy retains a cubic shape with obtuse corners and shows a core–shell structure with a core and two shells. We examined this core–shell Pt–Al nanoalloy by atomic resolution TEM (JEOL JEM-ARM200F) as shown in Figures 2d and 2e. The core (Figure 2d) shows a single-crystal particle with a diameter of approximately 10 nm. The lattice spacing between the {200} planes, 0.196 nm, is also in agreement with that of bulk Pt crystal. In contrast, Figure 2e demonstrates an inner shell of amorphous Pt–Al in which nanocrystals of several nanometres are embedded. Hence, the core–shell structure can be represented as having a 17-nm thick Pt–Al alloy shell surrounding a 10-nm Pt core. The outer shell (4–6 nm) may be alumina after exposure to air.[7] We found that an alumina shell is quite stable and can prevent Pt–Al nanoalloys from aggregating even at 500 °C. EDX revealed that the atomic contents of Pt and Al are 14.7% and 85.3%, respectively. Figure 2c is a TEM image of porous Pt nanoparticles after the wet-chemical etching of the core–shell Pt–Al nanoalloys by KOH solution overnight. From the TEM observation, some portion was found to collapse, and the particles were no longer cubes. The structure can be described as crosslinked "arms" with many "pores" among them. Note that a significant quantity of Al may remain, because Pt atoms should accumulate on the surface and locally block further Al dissolution. EDX shows that two metals remain in the porous nanoparticles, Pt and Al, with atomic content of 75.9% and 24.1%, respectively. This means that Al is not removed totally by chemical etching. Distribution of the porous Pt nanoparticles is estimated to be 40.6 ± 4.0 nm, the average value from over 100 measurements (Figure S3).[8] As shown in Figure 2f, the atomic-resolution TEM image for one pore indicates polycrystals with various lattice structures. After carefully calculating the lattice fringe in Figure 2f, we found various spacing for this pore structure: 0.196 nm for Pt{200}, and 0.218, 0.209, and 0.190 nm for Pt porous alloyed with a small quantity of Al in the sublayer.

To investigate the core–shell Pt–Al nanoalloy and porous Pt nanoparticles in more detail, scanning transmission electron microscope (STEM) images collected by a high-angle annular dark field detector attached to the atomic-resolution TEM were used to characterize the microstructure and chemical composition of core–shell Pt–Al nanoalloy and porous Pt nanoparticles. Figure 3 depicts the STEM images of core–shell Pt–Al nanoalloy and porous Pt nanoparticles and the compositional line profiles probed by EDX. The bright contrast in STEM is the Pt. The line scans marked "1" and "2" illustrate the core–shell Pt–Al nanoalloy through the center and outer layers, respectively. From line scan (1), one can observe that the Pt core is covered by two layers, a Pt–Al alloy shell and an alumina shell without Pt signals, which coincide with the TEM image in Figure 2b. Line scans (3) and (4) illustrate the compositional line profile of the porous Pt nanoparticles. The obvious difference is the decrease in intensity of Al not only in the center but also in the outer layer, indicating partial Al removal after chemical etching. The intensity of Pt shows an obvious ridge valley structure, where the valley corresponds to the pore structure (marked with hollow red arrows) and the ridge corresponds to the Pt "arms" in the porous Pt nanoparticles.

Finally, the electrocatalytic properties of the porous Pt nanoparticles were investigated with the methanol oxidation
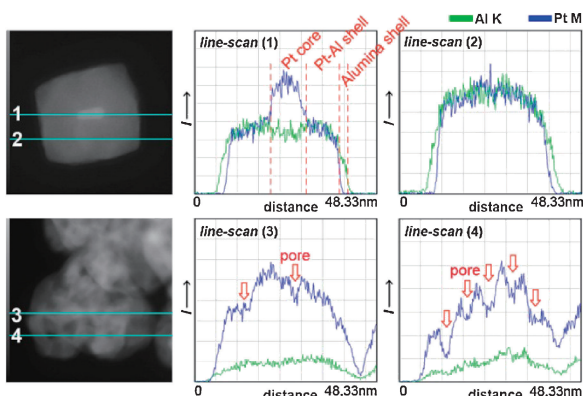
Figure 3. STEM images and compositional line profiles along the scanned line probed by EDX for core–shell Pt–Al nanoalloy and porous Pt nanoparticle.

reaction (MOR). Cyclic voltammetry was performed with a working electrode coated with the samples described above in a 0.5 M $H_2SO_4 + 2$ M CH_3OH electrolyte at a scan rate of $50 \, mV \, s^{-1}$ after purging with N_2 gas for 1 min and electrochemical cleaning. The working electrode was a glassy carbon electrode, 5 mm in diameter, coated with the electrocatalyst layer. Three milligrams of Pt was placed in 3 mL of ethanol containing 0.2 wt % Nafion solution suspended with sonication for 1 h. A 12-µL portion of this slurry was placed onto a glassy carbon electrode and dried in a vacuum oven at room temperature for 1 h. The counter and reference electrodes were a Pt wire and a saturated calomel electrode, respectively. To evaluate change in the catalytic activity, the exchange current density (J) of the MOR was calculated and normalized to the electrochemical surface area determined by H_2 adsorption.[3a] We compared the current density of our porous Pt nanoparticles with commercial Pt black without carbon support (Aldrich, with a diameter of 4 nm) and with a Pt catalyst on carbon support (Pt/C, Tanaka Kikinzoku, Japan, 40 wt %). As shown in Figure 4, porous Pt nanoparticle showed a higher current density ($10.2 \, mA \, cm^{-2}$) than commercial Pt black ($1.7 \, mA \, cm^{-2}$) and commercial Pt catalyst on carbon support ($4.5 \, mA \, cm^{-2}$). Because current density is sensitive to the orientation or crystallization of Pt on the surface, we consider that the enhanced electrocatalytic activity of porous Pt nanoparticles originates from the special porous structure and different absorption sites with longer Pt–Pt interatomic distance owning to the Al atoms in the sublayer, as indicated by atomic-resolution TEM (Figure 2f).

In conclusion, we have synthesized two types of novel materials, a core–shell Pt–Al nanoalloy and a porous Pt nanoparticle by selective deposition of Al on a large-sized Pt nanocube and wet-chemical etching of a Pt–Al nanoalloy, respectively. The Pt nanocube serves as a catalyst for dehydrogenation of alane and as the seed for Al crystallization. During the formation of the Al shell, Pt atoms diffuse into the Al layer
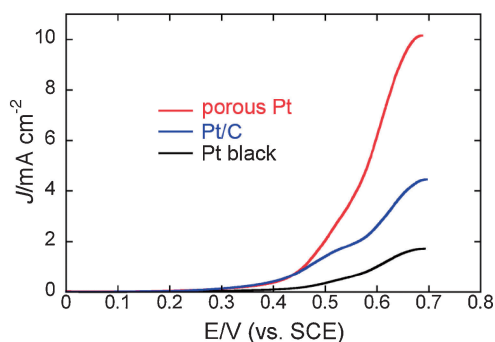
Figure 4. Current density of commercial Pt black (black line), commercial Pt/C (blue line), and porous Pt nanoparticles (red line).

to form a core–shell structure of the Pt–Al nanoalloy surrounding a Pt core. Chemical etching produces porous Pt nanoparticles with a catalytic activity higher than that of commercial Pt/C or Pt black. This method provides a possibility of combining both high surface area and the highly active facets for Pt nanoparticles.

References and Notes
1 For example: a) Z. Shen, M. Yamada, M. Miyake, *Chem. Commun.* **2007**, 245. b) K. M. Bratlie, H. Lee, K. Komvopoulos, P. Yang, G. A. Somorjai, *Nano Lett.* **2007**, *7*, 3097. c) *Electrocatalysis of Direct Methanol Fuel Cells: From Fundamentals to Applications*, ed. by H. Liu, J. Zhang, Wiley-VCH, **2009**. d) Z. Shen, Y. Matsuki, T. Shimoda, *Chem. Commun.* **2010**, *46*, 8606.
2 a) G. A. Somorjai, D. W. Blakely, *Nature* **1975**, *258*, 580. b) N. Tian, Z.-Y. Zhou, S.-G. Sun, Y. Ding, Z. L. Wang, *Science* **2007**, *316*, 732.
3 a) C. Wang, H. Daimon, T. Onodera, T. Koda, S. Sun, *Angew. Chem., Int. Ed.* **2008**, *47*, 3588. b) H. Song, F. Kim, S. Connor, G. A. Somorjai, P. Yang, *J. Phys. Chem. B* **2005**, *109*, 188.
4 Z.-Y. Zhou, Z.-Z. Huang, D.-J. Chen, Q. Wang, N. Tian, S.-G. Sun, *Angew. Chem., Int. Ed.* **2010**, *49*, 411.
5 For example: a) G. Surendran, L. Ramos, B. Pansu, E. Prouzet, P. Beaunier, F. Audonnet, H. Remita, *Chem. Mater.* **2007**, *19*, 5045. b) D. Yang, S. Sun, H. Meng, J.-P. Dodelet, E. Sacher, *Chem. Mater.* **2008**, *20*, 4677. c) X. Zhang, W. Lu, J. Da, H. Wang, D. Zhao, P. A. Webley, *Chem. Commun.* **2009**, 195.
6 M. Schrinner, M. Ballauff, Y. Talmon, Y. Kauffmann, J. Thun, M. Möller, J. Breu, *Science* **2009**, *323*, 617.
7 C. E. Aumann, G. L. Skofronick, J. A. Martin, *J. Vac. Sci. Technol., B* **1995**, *13*, 1178.
8 Supporting Information is available electronically on the CSJ-Journal Web site, http://www.csj.jp/journals/chem-lett/index.html.